

Tau Coupling Investigation Using Positive Wavelet Analysis

Linghai Lu¹, Michael Jump², and Michael Jones³
University of Liverpool, Liverpool, Merseyside, L69 3GH England, United Kingdom

¹Email: linghai@liv.ac.uk ; ²Email: mjump1@liv.ac.uk; ³Email: michael.jones@liverpool.ac.uk

Abstract

Investigation into motion guidance using τ theory primarily relies on the accurate calculation of the coupling term between the tau (time-to-contact) of the motion, τ , and its relevant so-called tau guide. However, the traditional approach is numerically unstable, requiring experience and skill, and has limited application when information is incomplete. A new approach based on positive wavelet analysis, combined with the new concept of a guidance element, has been proposed to deal with these issues. The desired τ -guide shapes form the mother wavelet and its scale is considered to be the manoeuvre period. The scale and positions of interest are found by searching the best local correlation with the whitened original signal. An inverse de-whitening process is used to approximately reconstruct the original signal. The adequacy of the proposed approach has been demonstrated on data from piloted simulation. Results show that the proposed approach is feasible, has better numerical stability and reliability, enhanced performance and wider application.

Nomenclature

a, b	=	scale factor and translational value
C	=	constant value
f	=	signal function
h	=	power number from fitting with the PSD curve
k	=	coupling constant between motion and guide
K	=	input-output gain
n, N	=	current and total number of the local extremes
t	=	time variable (s)
\hat{t}	=	distance normalized by duration of a manoeuvre
T	=	duration of a manoeuvre (s)
V_x, V_y	=	forward and lateral speed (ft/s; pixel/s)
W	=	Wavelet coefficient
x, \dot{x}, \ddot{x}	=	distance to go, velocity, and acceleration in the x direction (ft, ft/s, ft/s ² ; pixel, pixel/s, pixel/s ²)
\hat{x}	=	distance normalized by manoeuvre distance
y	=	distance to go in the y direction (ft; pixel)
δ_{1c}	=	lateral cyclic input (inch)
ξ	=	damping ratio
τ	=	optical τ , the instantaneous time to close on a goal or gap (sec)
$\dot{\tau}, \ddot{\tau}$	=	rate and acceleration change of optical τ
T_d	=	system time delay (s)
Φ	=	de-whitening signal
ψ	=	mother wavelet
ω	=	frequency point
ω_n, ω_d	=	natural frequency and forced frequency

Subscript

g	=	intrinsic τ guidance
i	=	iteration number

Symbol

\wedge	=	normalised terms
$*$	=	operation of complex conjugate

1. Introduction

Optical tau (τ) theory has been extensively investigated in recent research activities [1-3]. It is based on the premise that purposeful actions are accomplished by coupling the motion under the control of an observer with either externally or internally generated guidance sources – the so-called motion guides [1;4;5]. Motivated by its basis in visual perception, researchers have applied τ theory to flight control and handling qualities problems [2;6-9]. These applications are based on the hypothesis that, in terms of a visual guidance strategy, the overall pilot's goal is to overlay or close the gap between the perceived optical flow-field over the required flight trajectory. The pilot then works directly with optical variables to achieve prospective control of the aircraft's future trajectory. One of the first applications of τ -coupling to aircraft flight considered τ -guidance control strategies during a helicopter deceleration manoeuvre close to the ground [6]. An investigation of terrain-hugging flight reinforced the prospective control behaviour of helicopter pilots [2;7;10]. Similar results have been found by applying τ -guidance to the landing flare manoeuvre of fixed-wing aircraft [8;9] and to Boundary

Avoidance Tracking (BAT) Adverse Pilot Coupling (APC) phenomenon in the roll step manoeuvre [11].

Tau-guidance is achieved by using τ -coupling [1], that is, keeping the tau of one parameter in proportion to the tau of another. An example of this kind of coupling is shown later in the paper. Such motion is regulated by a coupling term, k . This parameter plays a vital role in τ -theory, describing the kinematics of the motion. Previous investigations using τ -theory, such as its application to aircraft [1;3], actually focus on exploiting and interpreting the values of k that are achieved. In these cases, the successful implementation of τ -theory primarily relies on an accurate calculation or estimation of the value of k . The traditional approach to obtain this value is simple. The parameter k is usually obtained through an optimization process, such as the classical linear least-square-error (LSE) method [12]. However, this approach suffers from deficiencies [11]. For instance, the LSE method has been found to be sensitive to the selected period over which the data is optimized. Its numerical stability is also vulnerable to the boundary conditions of the time period selected for the motion under investigation. Moreover, when the original data are incomplete or combined with severe oscillations, the LSE method will not usually be able to deal with the data satisfactorily.

To the author's knowledge, no effort has yet been made to address the issues, outlined above, with the application of τ -theory. This paper proposes a new approach, based on positive wavelet analysis (PWA) [13-15], to deal with these deficiencies. This special type of wavelet analysis is applicable to decomposing a signal using user-defined features, such as the form of a positive pulse used to analyse atmospheric turbulence [15], terrain analysis [16], and pilot workload qualification [17]. The concept of "positive" wavelets originates from the replacement of the traditional oscillatory wavelet [18] with a positive pulse that can be translated and dilated [13-15]. Positive wavelet analysis is similar in purpose to classical wavelet analyses; it detects the detailed features of a signal by using a process of correlation with translated and dilated versions of the basis function. However, this approach violates the admissibility condition [13]. To account for this, the original signal on which PWA is applied is reconstructed using an approximation approach.

The paper proceeds as follows. Previous approaches to τ -coupling analyses and their deficiencies are reviewed and discussed in Section 2. The detailed development of the new approach, with user-constructed wavelets, is presented in Section 3. Two

case studies where the proposed new approach is applied are provided for validation purposes in Section 4. Results from the previous and proposed new approaches are then compared. Finally, conclusions are drawn in Section 5.

2. Traditional Analysis Approach

2.1 Review of Tau Coupling Guidance

Tau theory is based upon the fundamental variable, tau (τ), the time-to-contact variable in the optical field [1],

$$(1) \quad \tau(x,t) = \frac{x}{\dot{x}}$$

where x is the motion gap to be closed and \dot{x} is the instantaneous gap closure rate. The term 'motion gap' refers to a perceived difference between the observer's current and desired target state. This concept was formulated by Lee [1] when modelling how animals control their movement prospectively through the cluttered environment close to the Earth's surface. The 'motion' gaps can be extended to take other forms, such as force (e.g. when taking a step whilst walking) or auditory signals (e.g. whilst playing an instrument or when singing a song), etc. [5]. In addition, the τ variable is hypothesised to be sensed directly by subjects, without the need for cognitive reasoning or computation for the motion to be perceived and controlled. This, it is supposed, is the result of natural evolutionary processes - movement guidance should be simple, rapid, reliable and biologically plausible. If this were not the case, the guidance process may be degraded by associated delays and noise contamination of lengthy computations or cognitive thought processes [1;5]. A number of examples offer evidence to support this hypothesis [1;4;5;7].

In reality of course, there are often two or more gaps required to be closed simultaneously, such as the coordination required between the lateral and forward motions (e.g. in the biological world, when closing on a prey animal) or forward and vertical motions, in order to achieve combined horizontal-vertical manoeuvres [19]. Two motions, $x(t)$ and $y(t)$, are said to be τ -coupled if the following relationship is satisfied,

$$(2) \quad \tau_y = k\tau_x$$

The coupling term k in Eq. (2) regulates the dynamics of the motions in the x and y axis systems. Tau coupling requires τ to be perceived. By keeping τ values of motion gaps in a constant ratio, τ -coupling

results in effective navigation through a power law (for $x < 0$, and $y < 0$),

$$(3) \quad y = C(-x)^{1/k}$$

The convention in τ -theory is to define motion gaps as closing from negative values to zero [1]. Tau-coupling can take two forms; extrinsic (x and y are physically observable) or intrinsic (x is physically observable while y is internally generated, potentially by the observer's neural system). The intrinsic motion gaps are assumed to be generated by internal sensory arrays, required when extrinsic variables are not available to guide movement, such as self-paced movement where only one motion is involved [5]. In this case, intrinsic guidance of movement, through a so-called τ -guide, τ_g , is hypothesized to be modelled through the relationship,

$$(4) \quad \tau_x = k\tau_g$$

τ_g guidance is therefore based upon the premise that an internally generated motion guide provides the stimulus onto which an externally perceived gap can be coupled. It can be shown that for general deceleration-to-stop motions, the natural intrinsic guide can take the form of either constant velocity, constant acceleration (e.g. hover to hover), or constant deceleration (e.g. braking) [2;5]. The detailed derivations of the motion laws are given in Appendix A (Table A1) for completeness.

In Table A1, the dressing ' \wedge ' indicates that the variables are normalised by T , the total duration of the manoeuvre, so that $0 < \hat{t} \leq 1$. Moreover, the constant velocity and deceleration guidance reflects the constant rate of change of τ_x with time, derived based on Eq. (4) [2],

$$(5) \text{ For constant velocity guidance } \quad \dot{\tau}_x = k$$

$$(6) \text{ For constant deceleration guidance } \quad \dot{\tau}_x = \frac{k}{2}$$

The significance of the constant acceleration or deceleration guides is suggested to stem from the influence of gravity on the movement of humans and animals during evolution [1;5], while constant velocity is mimicked by horizontal motions of thrown objects, at least in the short term. Experiments have verified the existence of the intrinsic τ information embodied in the nervous system [5], as well as the potential use of τ_g guidance in aircraft operations [6-9]. Furthermore, previous investigations have shown that humans and animals tend to adopt constant $\dot{\tau}$ strategies during the deceleration phase for visually guided movements, such as a hummingbird docking on a feeder tube,

automobile braking [20], helicopter quick-stop manoeuvres (where $\dot{\tau} = 0.5$ was common [6]), and during the flare manoeuvre in a fixed-wing aircraft [8;9].

2.2 Existing Issues with Calculating the Coupling Term

As shown Eq. (4) to Eq. (6), the coupling parameter k plays a vital role for guidance. It determines exactly how the motion gap closure will occur. It reflects the kinematics of a movement together with the duration of the manoeuvre (T) [2]. For an intrinsic τ -guide with a constant deceleration, the motion-gap closure with $k \leq 1$ ($\dot{\tau} < 0.5$) will ensure a 'stop' at the desired goal. In addition, the case when $k = 1$ corresponds to motion with a constant deceleration throughout the approach to the stop. Therefore, the study of the τ coupling will tend to focus on the investigation of the k values achieved. The accurate determination of the k value is therefore of the utmost importance in a tau-theory based analysis. As shown in Fig. A1, a small percentage variation in the value of k can represent a completely different kinematic motion.

The traditional procedure to obtain the k value is straightforward and reviewed here, taking the constant acceleration guide as an example. The shape of a typical motion gap closure rate is illustrated in Fig. 1. It can be seen, by comparing with rates of closure charts in Fig. A1 that this motion bears similarities to those curves generated by motion coupled to a constant acceleration tau guide. It is therefore of interest to establish the closest value of k that would generate such a motion.

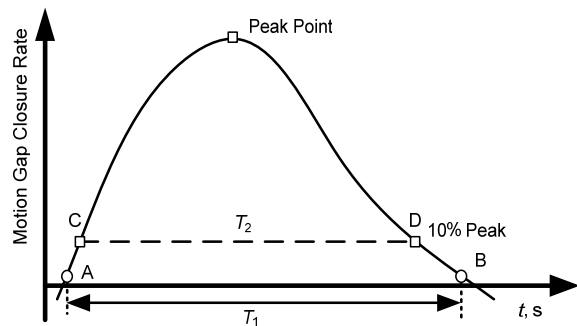


Fig. 1 A typical motion gap closure rate with constant acceleration guide

Two approaches have previously been implemented to calculate k value in Eq. (2). The procedures used have been summarised in Fig. 2.

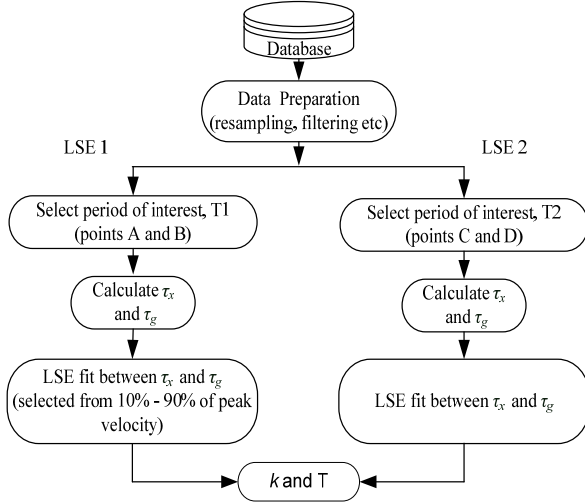


Fig. 2 Flow charts of previous approach used to calculate coupling term k values

As shown on the left-hand side of Fig. 2, the first approach (LSE1) determines the duration of the manoeuvre (T_1) based upon the zero-crossing velocity

information of the motion (i.e. the period T_1 between points A and B in Fig. 1). Afterwards, the τ_x curve can be calculated based on Eq. (1) with the motion gap and its closure rate. Moreover, with the available T_1 value, τ_g in Eq. (4) can now also be obtained with the related formula in Table A1. For instance, the following equation is adopted for the constant acceleration guide.

$$(7) \quad \hat{t}_g = -\frac{1}{2} \left(\frac{1}{\hat{v}} - \hat{t} \right)$$

The LSE algorithm is then applied to the user-selected part of the $\tau_g - \tau_x$ curve to find the k value. Alternatively, a second approach (LSE2) can be used whereby the sample time period is selected based upon a smaller subset of data available to allow the tau guidance to become more firmly established in the motion. For example, 10% of the peak velocity was used as a threshold value in the analysis of data in Ref. [2]. This corresponds to period T_2 in Fig. 1. The $\tau_g - \tau_x$ curves, calculated from point C to D, are now used for the curve fitting process in this case.

Although this whole process is simple and easy to implement, this approach suffers from a number of issues. Firstly, the k value achieved is highly sensitive to the selected manoeuvre period. This issue is illustrated in Fig. 3.

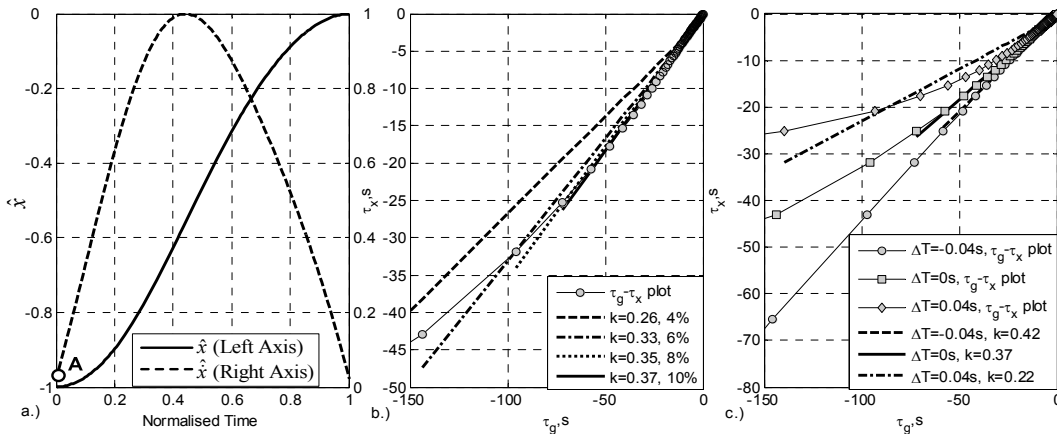


Fig. 3 Illustration of the sensitivity of the k value to the selected fitting range (b) and manoeuvre period (c)

The same normalisation procedure used for Table A1 has been applied to the case shown in Fig. 3. The percentages in the legend of Fig. 3b represent the start and end points of the manoeuvre in terms of the peak velocity in Fig. 3a (i.e. the period T_2 between points C and D in Fig. 1). As shown in Fig. 3b, in which τ_g is calculated using the constant acceleration

guide, the different selection of the peak velocity at which the data is cropped has a significant influence on the k values achieved. The cropping procedure is used mainly to remove the sparse information (widely distributed cycle in the $\tau_g - \tau_x$ curve in Fig. 3b) that can lead to poor LSE fitting. The k value at 4% of peak velocity is about 30% different from the one where the

data is cropped at 10% of the peak velocity. For this case, increasing the percentage of the velocity at which the data is cropped seems to lead to a better fit in Fig. 3b. This is due to the meaningful information being located mainly in the smaller negative amplitude of the $\tau_g - \tau_x$ curve, as reflected in the high distribution density of the cycles within the region close to the origin in Fig. 3b. This, of course, will lead to an increased loss of information that could otherwise be used in the optimisation algorithm. Fig. 3c depicts the large variation of the k value associated with a minor variation of the period of the manoeuvre, T_1 , selected. This is equivalent to slightly adjusting the initial position of the manoeuvre (point A in Fig. 3a). The consequent τ_g curve, which depends only on the T_1 variable as shown in Table A1, will therefore be changed. Moreover, the slight adjustment of the start of the manoeuvre brings in the large changes in the initial velocity. This also will have an effect on the τ_x curve. These two factors result in the significantly different distribution of the $\tau_g - \tau_x$ curves in Fig. 3c. Therefore, this case shows the difficulty in obtaining a reliable k value using the traditional approach.

The second approach (LSE2) was proposed to address the sensitivity of the k value to the selection of the period T_1 [2]. As shown on the right-hand side of Fig. 2, the period T is fixed by referring to a predefined threshold velocity (e.g. the period from C to D at 10% of peak velocity shown in Fig. 1). The $\tau_x - \tau_g$ curves are then calculated within this fixed period. Afterwards, the k values are obtained with the same LSE fitting algorithm used for the LSE1 approach. However, in practice, LSE2 still needs the user to tune a reasonable threshold velocity to reach the convergence of the LSE algorithm. This manual process, again, leads to a variation in the k values that can be obtained. Fig. 4, with the same data source as

in Fig. 3a, illustrates how the different peak velocity cut-off percentages selected leads to a variation in k .

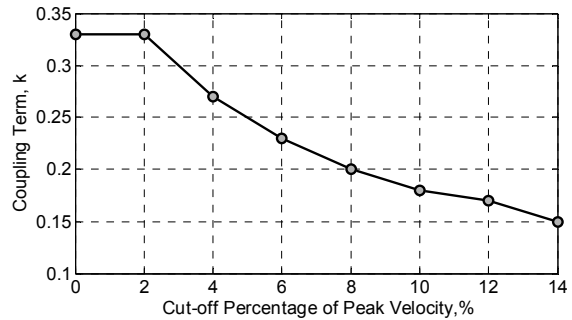


Fig. 4 Coupling term k variation with cut-off percentage of peak velocity

The results in Fig. 4 show that k values decreases from 0.33 to 0.15 as the cut-off percentage increases for 2 to 14% of the peak velocity. Therefore, this “tuning” may lead to a misinterpretation of the obtained k value, the user believing that this might lead to a better convergence of the LSE algorithm (by removing the sparse part of in the $\tau_g - \tau_x$ curve in Fig. 3b). This user-involved process cannot guarantee that it will result in the “true” k value that actually reflects or captures the pilot’s guidance strategy.

Apart from the difficulty in selecting the range of data, experimental results do not always contain the characteristic smooth bell shape of the velocity shown in Fig. 3a. Such data profiles are desirable as they generally result in numerically stable and well converged k values because of a good fit with the theoretically derived shapes shown in Fig. A1(c, f). However, in practice, such motion gap profiles may not exist at all, or they might be incomplete or combined with oscillations, as shown in Fig. 5.

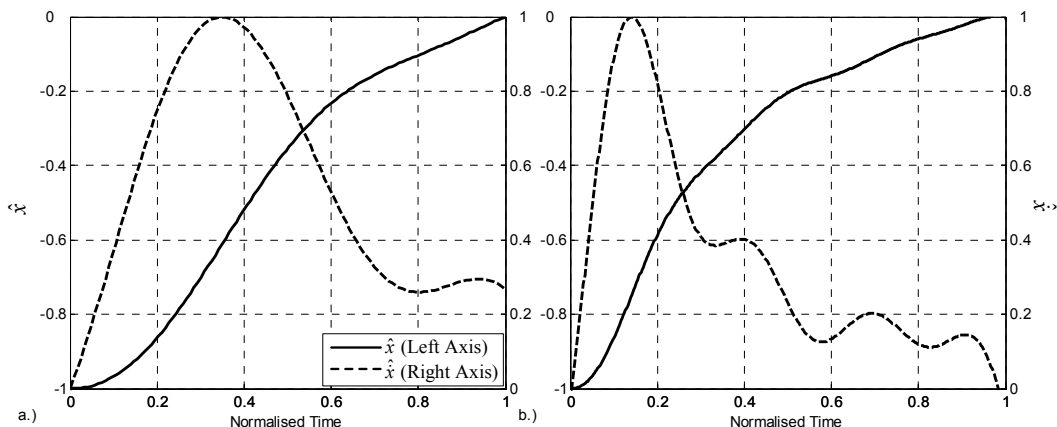


Fig. 5 Illustration of two special Accel-Decel cases

Beyond these issues of manual intervention, the motions that result from tau guidance have specific boundary conditions. The current method suffers when the measured motion does not conform to these boundary conditions. For example, Fig. 5a displays an example of a 'good' initial Accel-Decel bell shaped curve describing the velocity of the manoeuvre, but which then (after $t = 0.8$ s) becomes flattened off. This shape is not consistent with any curve shown in Fig. A1(c, f). Furthermore, its end velocity is about 25% of its peak velocity which is well above the threshold that is typically adopted for such an analysis (10%). Therefore, according to the traditional methodology, the data displayed in Fig. 5a would represent a case that was difficult, if not impossible to analyse in a meaningful way using tau theory. Fig. 5b reflects an even more complex situation displaying oscillations in the vehicle's velocity prior to reaching the desired goal. Although its velocity represents an approximate bell shape (Fig. A1f), it has been found difficult to reach a reliable k value using the traditional approach.

Finally, one further limitation in the research conducted so far is that the motions analysed have been restricted to investigation one tau guide at a time. There has been no scope to investigate the combination of tau guides to represent the potentially more complex motions that result from real measured data.

As a consequence of all of the identified issues, a new methodology to address these drawbacks required to be developed. The creation of such a method is the subject of the remainder of this paper.

3. Tau Coupling Based on Positive Wavelet Analysis

An alternative approach to obtain the tau guide coupling parameter, k , based on PWA[13;14;17] is proposed in this paper to address the issues highlighted in the previous Section. The whole procedure can be divided into the following three steps;

1. Decompose the motion data into individual but possibly differing guidance elements;
2. Perform a positive wavelet transform on the motion gap and
3. Perform an approximate reconstruction of the motion gap.

Each of these steps will be discussed in more detail in what follows.

Step 1: Decompose Motion Data into Guidance Elements

The research reported in Refs. [3;17;21] describes the three functions of flight management and control – there are the two short-term activities of stabilisation and guidance, and one longer term activity, navigation. The navigation function is normally described as the means of closing the current and a goal position, and is usually not a concern for the pilot because the position information is known in advance. The pilot control activities are more related to stabilisation and guidance functions. A pilot normally performs these two functions simultaneously during flight. The stabilisation function refers to the continual correction efforts of a pilot to avoid deviating from the desired flight path [2]. This function is considered to be conducted within the range of high frequency control activities (1 – 2.5 Hz) and affected by the aircraft internal dynamics as well as the pilot gain [17;21]. The guidance process is generally located within a lower frequency band (< 0.5 Hz) and mainly involves the avoidance of ground and obstacles. The three intrinsic τ guides – constant acceleration, velocity, and deceleration, reviewed above, can be thought of as providing the guidance function through τ coupling [2]. Therefore, the study of intrinsic τ guide is carried out in the frequency range [0, 0.5 Hz] for the purposes of this paper to maximally eliminate the stabilisation function.

As mentioned in Section 2.2, the traditional approach to τ -coupling analysis has difficulty in dealing with the case in Fig. 5b in that that manoeuvre is assumed to be guided by only one intrinsic τ guide. To solve this problem, the intrinsic τ guide is extended and the idea of a guidance element is proposed. Guidance elements are presented as three kinds of intrinsic τ guide. A guiding process is considered to be composed of a series of guidance elements, with a single element used during a certain period. This is similar to ADS-33E, which divides an operation into many missions that in turn consists of a series of continuous mission phases and task elements (MTEs) [2;22]. Moreover, the initial and terminal speeds for an intrinsic τ guide are no longer required to be zero, in contrast to the manoeuvres used in previous research efforts, such as hover-to-hover or deceleration-to-stop [2]. Each guidance element is determined from the acceleration zero-crossing information. For example, the Accel-Decel manoeuvre in Fig. 5b is considered to have four guidance elements, as illustrated in Fig. 6.

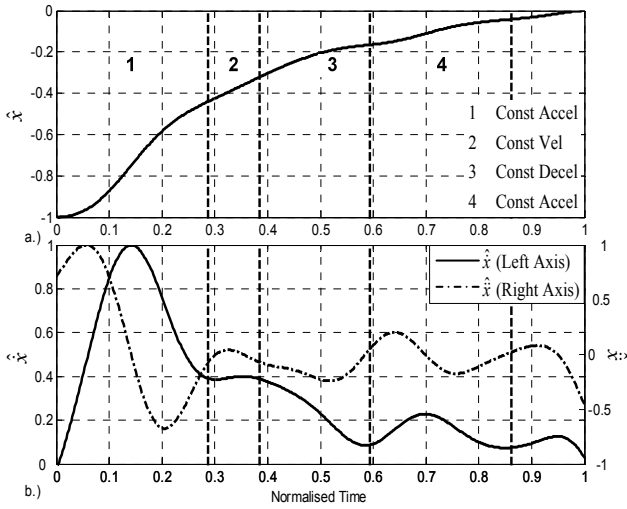


Fig. 6 Decomposing a signal into guidance elements based on acceleration information

The first guidance element (marked as 1 in Fig. 6a) is the constant acceleration guide, reflected in the Accel-Decel shape of the gap closure acceleration in Fig. 6b. The second period is considered to be governed by a constant velocity guide, selected with regard to the nearly zero closure acceleration in this period. The third period is assumed to be a constant deceleration guide, followed by the fourth, a second constant acceleration guide. As noted in Fig. 6a, the first constant acceleration guide terminates with 41% of its peak velocity. Furthermore, the third constant deceleration guide does not finish with zero velocity and the constant acceleration guide of phase 4 also initiates and ends with a non-zero velocity. The shapes of the motion gaps and their closure rates for these four guidance elements are consistent with those in Fig. A1, with the exception of initial and end conditions. The proposed new approach using positive wavelet transforms will now be applied to each guidance element.

Step 2: Positive Wavelet Transform of the Motion Gap

The traditional continuous wavelets transform is defined as, [18]

$$(8) \quad W(a,b) = |a|^{-1/2} \int f(t) \psi^* \left(\frac{t-b}{a} \right) dt$$

in which $a (> 0)$ is scale factor, $b (\in \mathbb{R})$ is translational value, $f(t)$ is a given signal, and $\psi(t) \in L^2(\mathbb{R})$ is the mother wavelet. The symbol '*' represents operation of

complex conjugate. In addition, the daughter wavelets, $\psi_{a,b}(t)$, are defined as,

$$(9) \quad \psi_{a,b}(t) = \frac{1}{\sqrt{a}} \psi \left(\frac{t-b}{a} \right)$$

If the signal $f(t)$ needs to be reconstructed perfectly through inverse wavelet transform, the following admissibility condition needs to be satisfied,

$$(10) \quad \int \psi(t) dt = 0$$

For positive wavelet analysis, it is of interest to decompose a signal and then reconstruct it approximately [14;17]. Therefore, the mother wavelet is constructed violating the admissibility condition in Eq. (10), similar to the positive pulse used to analyse pilot workload qualification [17]. In addition, the signal $f(t)$ is pre-whitened to make its power spectral density (PSD) independent of frequency [13;14;17]. Hence, the significant information in the signal can be better localised through the correlation process in Eq. (8). The procedure used for whitening $f(t)$ is shown in Fig. 7 where ω is the frequency variable.

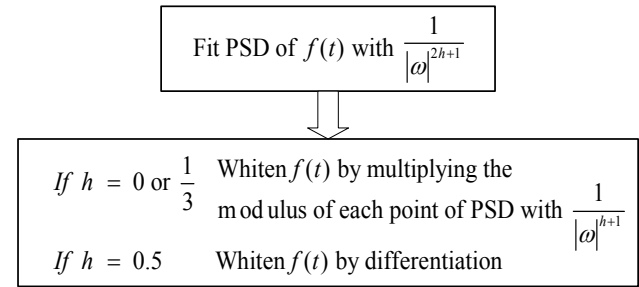


Fig. 7 The procedure for whitening the signal $f(t)$

In practice, the position and attitude signals normally follow the PSD distribution with $h=0.5$ and their rates with $h=0$ [13;17]. The atmospheric turbulence is found to be $h=1/3$ [15]. The signal $f(t)$ for the optical tau applications in this paper is either position or attitude information. Therefore, $h=0.5$ was selected for the whitening process in this paper.

After the signal $f(t)$ is whitened, the analysing wavelet $\psi(t)$ is constructed under the shape of the normalised motion gap closure rate. Taking the constant acceleration guide as an example, its formula cited from Table A1 is defined as,

$$(11) \quad \hat{x} = \frac{2\hat{t}}{k}(1-\hat{t}^2)^{\frac{1}{k}-1}$$

Eq. (11) shows that, the dynamic characteristics of a motion, if guided by an intrinsic τ guide, are all determined by the coupling term (k) and the duration of the motion (T , used for normalising \hat{t}). If the value (k) is determined, the shape of the normalised motion gap (\hat{x}) as well as its first and second order derivatives will be fixed, as shown in Fig. A1. Moreover, its amplitude and period can be uniquely tuned by T , which functions as the scale (a) in Eq. (9). Therefore, the positive analysing wavelet for the constant acceleration guide used in this paper based on Eq. (9) is described as,

$$(12) \quad \psi_{T,b}\left(\frac{t-b}{T}\right) = \frac{1}{\sqrt{T}} \frac{2(t-b)}{kT} \left(1 - \left(\frac{t-b}{T}\right)^2\right)^{\frac{1}{k}-1}$$

Three additional points have to be made about the wavelet form presented in Eq. (12). The first concerns the variable k . The form presented provides an infinite cluster of wavelets, each corresponding to one k value. A numerical algorithm has to be developed to find the optimum value. The second point, as mentioned earlier in the paper, is that this form fails to satisfy the admissibility condition of Eq. (10). This means that the original signal cannot be reconstructed without losing any information. However, for the approach presented, it is of more interest to detect the most correlated part of the signal with the designed positive wavelet. Then, based on the related T and k values, the original signal $f(t)$ can be approximately reconstructed, depending only on the local maxima and minima information of Eq. (12). Finally, compared with the classical wavelet techniques (e.g. Daubechies wavelets and Gaussian family wavelets that have good localization in the both time and frequency domains [18]), PWA tends to focus more on the time domain – the correlation of shapes between a signal and a scaled wavelet. This allows the users to have

more freedom to investigate the signal shapes of interest.

With the whitened signal and constructed wavelet, the wavelet transform is performed using Eq. (8) on one guidance element. In the time-scale plane, the local maxima and minima points (T_i and b_i) are recorded for the next-step, signal reconstruction.

Step 3: Approximate Reconstruction of the Motion Gap

Because signal $f(t)$ is whitened before the wavelet transformation, an inverse de-whitening process is required to reconstruct this signal that will have same shape as the previous. This de-whitening process is applied to the wavelet of Eq. (12). Furthermore, the signal $f(t)$ has been whitened ($h=0.5$) to have a flat PSD distribution that suggests the associated de-whitening process is simply integration [13]. Therefore, for the de-whitening component, $\Phi(t)$, the shapes of Fig. A1(c) can be selected for the constant acceleration guide as follows,

$$(13) \quad \hat{x} = -(1-\hat{t}^2)^{1/k}$$

and then the formula used to reconstruct $f(t)$ can be described as,

$$(14) \quad f(t) \approx \sum_{i=1}^N n_i \Phi\left(\frac{t-b_i}{T_i}\right) = \sum_{i=1}^N n_i \frac{1}{\sqrt{T_i}} \left(1 - \left(\frac{t-b_i}{T_i}\right)^2\right)^{\frac{1}{k}}$$

in which N is the number of local extremes selected from the time-scale plane. An orthogonalization process is adopted to remove redundancy of the N^{th} -dimension basis space constructed from $\Phi(T_i, b_i)$ in Eq. (14) [12]. After the orthogonalization process, the coefficients n_i are found by a linear minimum-square-error approach by fitting with the signal $f(t)$.

The above three steps are summarised in Fig. 8 for clarity.

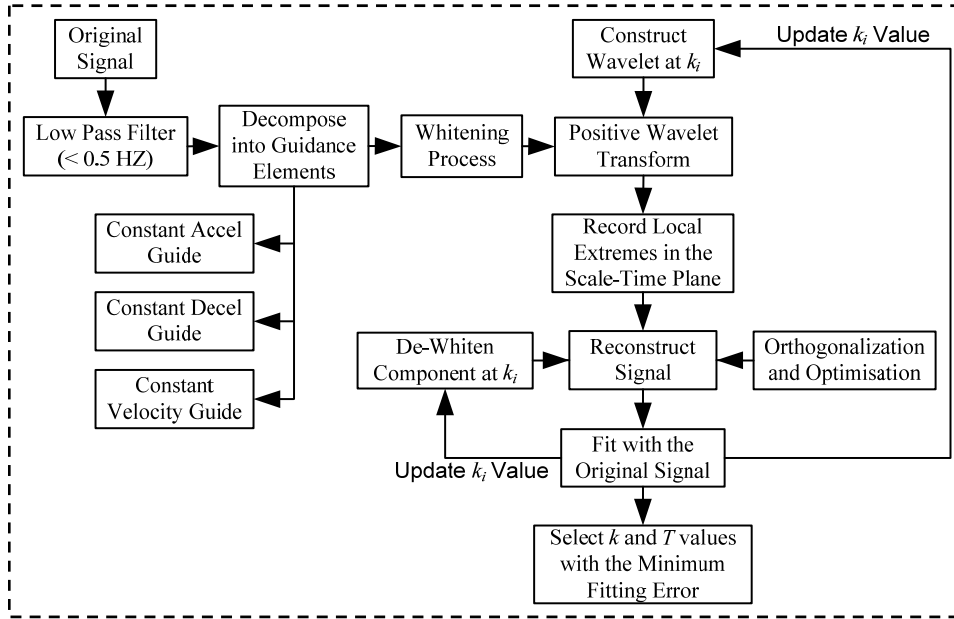


Fig. 8 Flow chart of PWA based on τ theory

Finally, the main differences between the previous (LSE 1 and LSE 2) and proposed approach (Positive Wavelet) are summarised in Table 1.

Table 1 Comparison between the LSE and PWA approaches

Items	LSE1	LSE2	Positive Wavelet
Theory	Classical optimisation algorithms by linearly fitting with the $\tau_g - \tau_x$ curves, e.g. the linear LSE method.		Positive wavelet analysing first based on the best correlation with the whitened signal, and then on the de-whitened signal. It is actually an approach that searches for the best fit with the user-defined shape.
Calculation of T	Manually selected and then slightly tuned around the two zero-crossing points of the motion gap closure rate.	Fixed by referring to a threshold velocity that need to be tuned in practice for convergence or better fitting	Automatically determined by the correlation algorithm (the optimised scale value) before the de-whitening phase.
Calculation of k	Optimisation on the user-selected parts of the τ_g and τ_x curves (cropped by a user).	Optimisation on the τ_g and τ_x curves	Optimisation of the root-mean-square (RMS) error between the reconstructed signal and the original signal.

4. Application and Validation of the New Approach

Two sets of experiments were conducted using The University of Liverpool (UoL)'s flight simulators [23;24]

as part of a wider set of test campaigns to develop tools and techniques to detect and alleviate Rotorcraft Pilot Couplings (RPCs). The data obtained has also been used to validate the new approach developed

above. The results from these applications are presented in this Section.

4.1 Mission-Task-Element Manoeuvres

The new methodology was first applied to results from three MTEs: Accel-Decel (AD), Vertical Manoeuvre

(VM), and Roll-Step (RS) manoeuvres either directly taken or adapted from ADS-33 [22]. Their individual layouts are shown in Fig. 9.

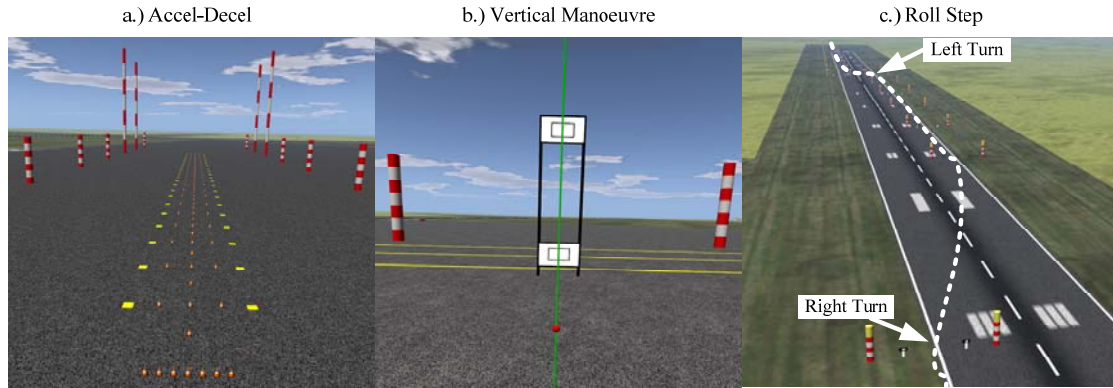


Fig. 9 Layout of MTE manoeuvres used to validate the wavelet approach

The three manoeuvres are described in more detail below:

- **Accel-Decel** (Fig. 9a): The pilot's task is to accelerate the aircraft to a target airspeed of 40 kts. The second phase of each MTE requires deceleration back to a stabilised hover at the marked end point, 700 ft from the start point.
- **Vertical Manoeuvre** (Fig. 9b): The manoeuvre commences in a trimmed hover-condition at the lower hover board, with the pilot required to reposition the aircraft vertically to a stable hover condition at the upper hover board. The simulation run is stopped when the stabilised condition is reached again at the lower hover board after initiating a descent. Two hover boards, positioned 25 ft apart and the inner (± 3 ft) and outer (± 6 ft) boxes, define the desired and adequate performance respectively. The course consists of poles sighted around two hover boards to provide the pilot with a visual cue. Each stripe on the poles represents a 10 ft height increment. This paper will investigate both the ascent (from bottom to top) and descent (in opposite direction) phases of the manoeuvre.
- **Roll Step** (Fig. 9c): Both sides of a 200 ft wide runway are flanked by a series of coloured gates, located 500ft apart. Depending on flight mode and speed, the pilot is required to fly through an ordered series of these gates which form the roll-step task. The manoeuvre requires the pilot to traverse the runway over the specified distance.

The manoeuvre starts with a constant forward flight speed lined up with the left edge of the test course at 30 ft above ground level. This paper will investigate both right (from left edge of the runway to the right one) and left (in opposite direction) traversing accel-decel processes.

These MTE tests were conducted with the FLIGHTLAB BO105 rotorcraft model developed at the UoL [25]. The MTEs were conducted on the UoL's HELIFLIGHT-R flight simulator shown in Fig. 10.



Fig. 10 HELIFLIGHT-R Research Simulator in the UoL [24]

HELIFLIGHT-R has a reconfigurable cockpit, capable of housing 3 seats; a pilot, co-pilot and flight engineer. The simulator has dual controls in collective, cyclic and pedal channels. The facility features a 12 ft

diameter dome with three HD LCoS projectors. These provide a blended $210^\circ \times 70^\circ$ field-of-view.

For experimental purposes, two time delays (τ_d): 0 ms and 200 ms, were introduced to the longitudinal cyclic control path for the AD MTE. Four time delays (τ_d): 0 ms, 100 ms, 200 ms, and 300 ms, were introduced to the collective control for the VM MTE and on the lateral cyclic for the RS MTE. Moreover, each time-delay configuration test point was conducted at least three times. The first run was used to help the subject to become familiar with the experimental set-up and is thus ignored for the analysis in this paper. In addition, the constant acceleration guide is applied to all of these MTEs due to the Accel-Decel nature of these manoeuvres.

As well as the new proposed methods, the LSE2 methodology, with the threshold of the 10% peak velocity, as shown in Fig. 1, is adopted for comparison because its wider application. The left-hand side of the $T_g - T_x$ curve, shown in Fig. 3b, has had to be cropped by a further 3% of peak velocity to enhance the convergence of the LSE optimisation algorithm. Otherwise, the LSE2 failed to achieve convergence for a few of the cases being investigated. Finally, four test pilots: A, B, C, and D, have been involved in the tests. The results from the LSE2 and the proposed methodology (PWA) are compared in Fig. 11 to Fig. 13.

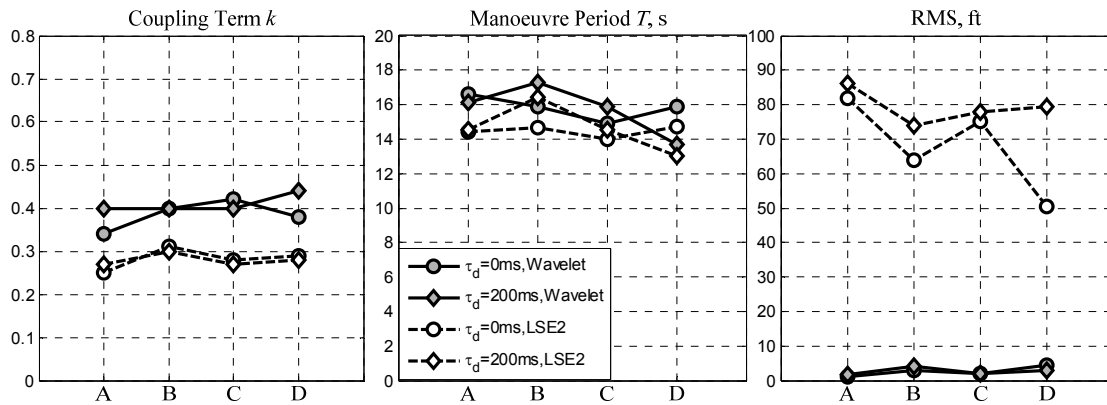


Fig. 11 Comparison of results from LSE2 and Wavelet approach for Accel-Decel MTE

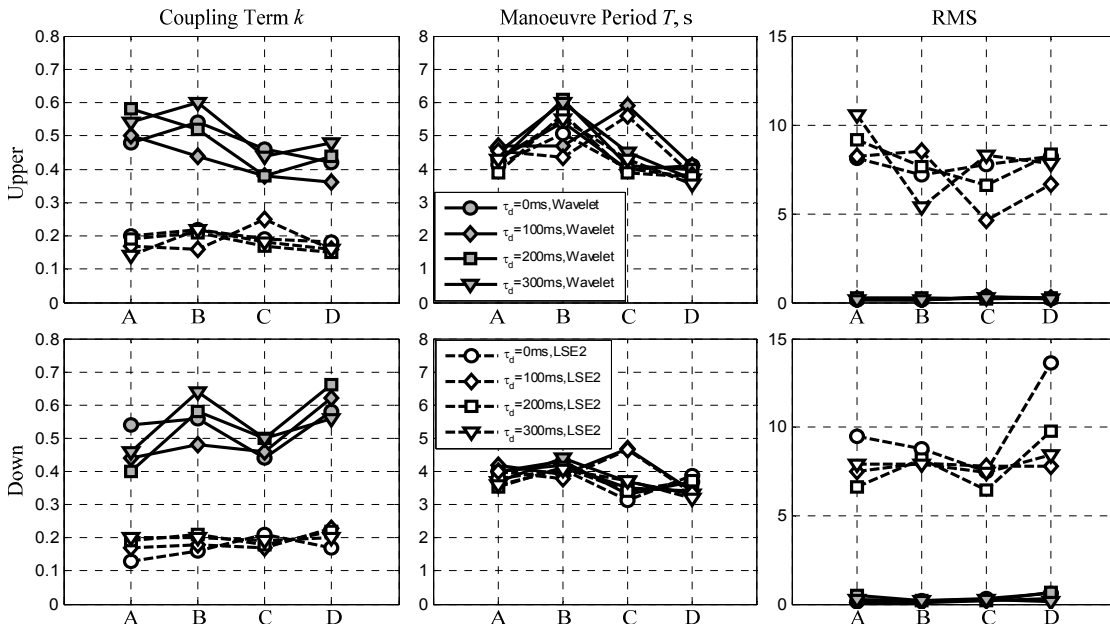


Fig. 12 Comparison of results from LSE2 and Wavelet approach for Vertical-Manoeuvre MTE

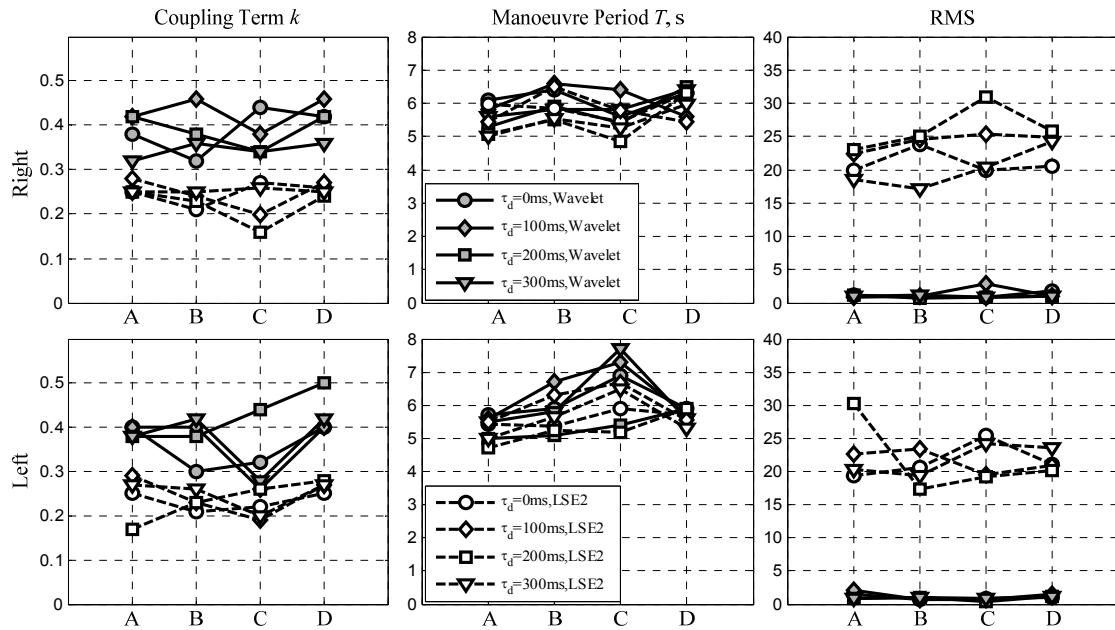


Fig. 13 Comparisons of results from LSE2 and Wavelet approach for Roll-Step MTE

Fig. 11 to Fig. 13 show that the values of the manoeuvre period T obtained using both LSE2 and the PWA approaches are close, generally within 15% of each other, regardless of the control channel, time delay and pilot used. However, initial and end positions for each case between these two methods may be different in that the T values from the new approach are automatically determined, in contrast to those fixed from the previous method. For the VM MTE in Fig. 12, it appears that the four pilots take an average of 0.8 s longer when traversing upwards than downwards. However, this timing difference is not reflected in the RS MTE in Fig. 13 because there is no timing limitation on the right or left traversing process.

The k values from these three MTEs also show consistency in terms of each pilot, the variation being generally within 15%. This implies that each pilot prefers to maintain a similar constant acceleration guide strategy to accomplish each MTE, the time delay having almost no effect on the k values (and hence the guidance strategy) obtained. These results provide strong evidence for the hypothesis that the k value is connected to the subject's control behaviour [2] as reflected in Eq. (4). Moreover, the k values from the LSE2 approach show less variation than those obtained using the new wavelet method. However, the k values of the new approach are larger than those of

the old, around twice the size in the AD and RS MTEs and nearly three times the values for the VM MTE. The different results of the same case from the different approaches can lead to completely different conclusions being drawn about the control strategy being used. For example, the k values with $\tau_d = 100$ ms in the VM MTE (down) in Fig. 12 are 0.62 (PWA) and 0.23 (LSE2), respectively, which represent two completely different control strategies. The k value equal to 0.62 indicates that the subject impacts the desired goal with a residual velocity and k equal to 0.23 suggests that the subject stops before reaching to the goal [11].

The question naturally arises as to which set of results are more correct. This requires a further check on the RMS values between the original signal and the one reconstructed from the calculated k value. All of the corresponding RMS values from the LSE2 approach from Fig. 11 to Fig. 13 are far larger than those from the PWA. This indicates that the signals reconstructed from the calculated k value with the LSE2 approach have a poorer fit with the original signal, although their k values appear to be more consistent. The comparison between the original signals and the constructed signals from both the LSE2 and PWA approaches for the AD MTE are plotted in Fig. 14 and Fig. 15 for to illustrate this point.

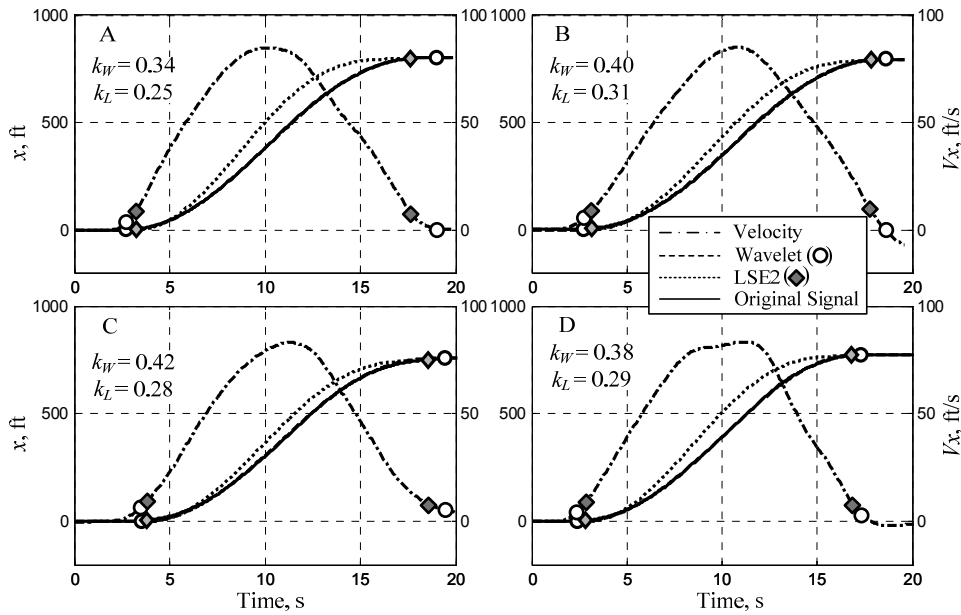


Fig. 14 Comparison of period selection and quality of fit ($\tau_d = 0\text{ms}$, Accel-Decel)

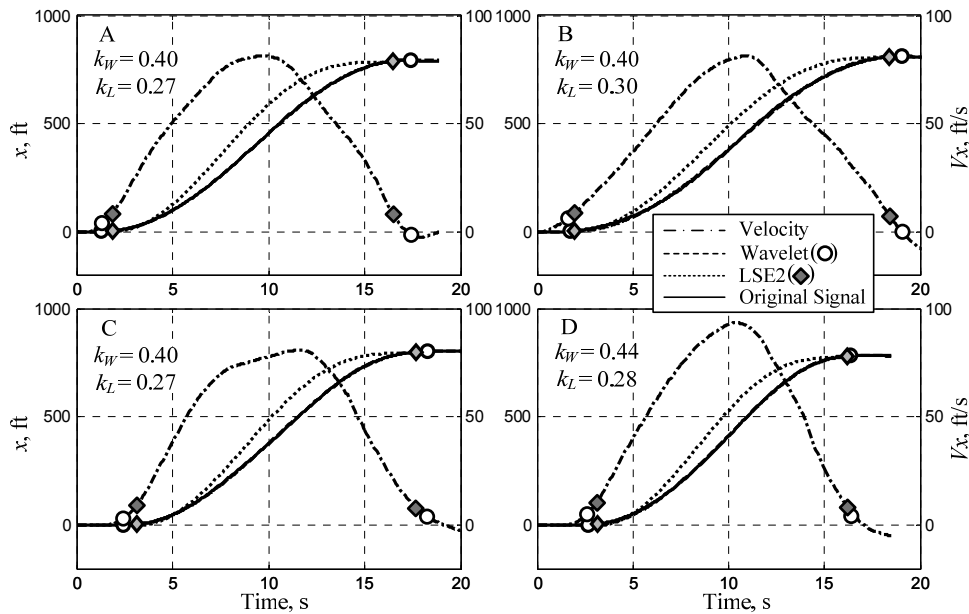


Fig. 15 Comparison of period selection and quality of fit ($\tau_d = 200\text{ms}$, Accel-Decel)

The variables k_L and k_W are the coupling term values obtained from LSE2 and PWA approaches respectively. As shown in the marked k values in Fig. 14 and Fig. 15 (or the lines in Fig. 11), each approach has achieved consistent k values, over different pilots, with the different τ_d values. However, the fit between the constructed signals with the k values from the LSE2 approach are not as good as those from the

PWA approach. It seems that even for the similar k values, the new approach has reached a far better fit with the original signal, as shown in the right axis of in Fig. 14 and Fig. 15, or by the smaller RMS values in Fig. 11. The better fit indicates that the PWA is more representative of reality. The main reason for the difference in fit due to the difference in the T values obtained. As mentioned above, the T value from the

PWA approach is automatically and optimally determined. Moreover, as reflected in the velocity curves in Fig. 14 and Fig. 15, the information used in the LSE2 approach (diamond symbols) is reduced when compared to the PWA method (circle symbols). The trends in the results can be observed to be similar for the other two MTEs. Therefore, in spite of appearing to be more consistent, the k values from the LSE2 approach may be not the “actual” ones that reflect the pilot’s control guidance strategy adopted and the values from the method proposed in this paper (PWA) present a more accurate representation of reality. For example, for the Accel-Decel cases, k values (all < 0.5) from both approaches have shown that a similar guidance strategy to initiate the deceleration is used. Therefore, in spite of being different from the PWA values, interpretation of the k values from LSE2 may be applicable. However, this is not the case for the Vertical Manoeuvre (Fig. 12) and the results from the LSE2 will be misleading. As discussed above, the k values (all < 0.5) from the LSE2 indicates the pilots elect to initiate the deceleration earlier in the manoeuvre. The conclusion is drawn differently from most cases (>0.5) shown in Fig. 12 that the pilots operate in the opposite way. These results again show the better numerical performance and more reliable conclusion achieved by the new approach developed in this paper.

4.2 Investigation of Pilot Control Activity Adaptation

A second set of data have been used to test the PWA method for tau coupling analysis. The aim of this experiment was to investigate the adaptation of pilot control activity when the dynamic configuration of the controlled system is varied [3]. The experiment configuration for this test is illustrated in Fig. 16.

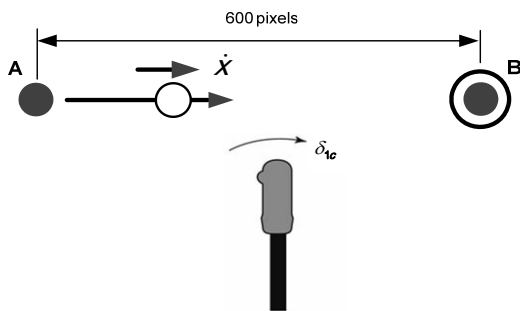


Fig. 16 Illustration of moving ball from left to right [3]

This experiment was conducted by Pilot A on the UoL’s HELIFLIGHT simulator [23;24] shown in Fig. 17.



Fig. 17 External and internal views of HELIFLIGHT Research Simulator in the UoL

HELIFLIGHT, shown in Fig. 17, sits on a six degree-of-freedom motion base and features an enclosed pilot station with five outside world and one instrument panel visual channels. The application of PWA to the results obtained from this experiment is presented in this Section.

The task was to move the ball from the left position (A) to the right position (B) across the screen using the lateral cyclic stick. Having reached the correct screen position, the pilot was required to hold the ball within the target circle for three seconds. The dynamics between the lateral cyclic input (δ_{1c}) and the ball was modelled as a second-order system

$$(15) \quad \ddot{x} + 2\zeta\omega_n\dot{x} + \omega_n^2x = \omega_n^2K\delta_{1c}$$

in which ω_n is the natural frequency, ζ is the damping ratio and K is the input-output gain (5.2 for this experiment). Furthermore, the movement of the ball is driven by the rate of flight path (\dot{x}). For the adopted axis in Fig. 16, the position A is considered to be the origin and the position B is 600 pixels away from A in the screen. The motion gap is defined to be the negative distance from the current point to point B in pixels.

The dynamic configuration of the controlled system was changed, by adjusting ω_n and ζ values in Eq. (15). These parameters were always tuned away from the reference configuration - $\omega_n = 4$, $\zeta = 0.7$ to ensure a better comparison among the different configurations. For example, when having finished a new configuration, the subject was asked to retake the reference configuration one time before commencing

with the next new set of dynamics parameters. For each configuration, the coupling term associated with the constant acceleration intrinsic τ guide (e.g. in Eq. (4)) reflected the control strategy the subject took. Therefore, this again shows the importance of accurately and reliably calculating the coupling term value to meet the objective of this experiment.

The aims of the current paper are to propose a new methodology that provides increased performance in

terms of the application of tau coupling analysis when compared to previous methods, not to investigate the original objectives of this experiment. Therefore, eleven configurations from the available database were selected for investigation here. Moreover, the data used have been filtered with a low-pass filter (0.5 Hz) to remove stabilisation control effort, especially when arresting the ball at position B [3]. The T and k values obtained from the data using both the LSE2 and PWA are presented in Fig. 18.

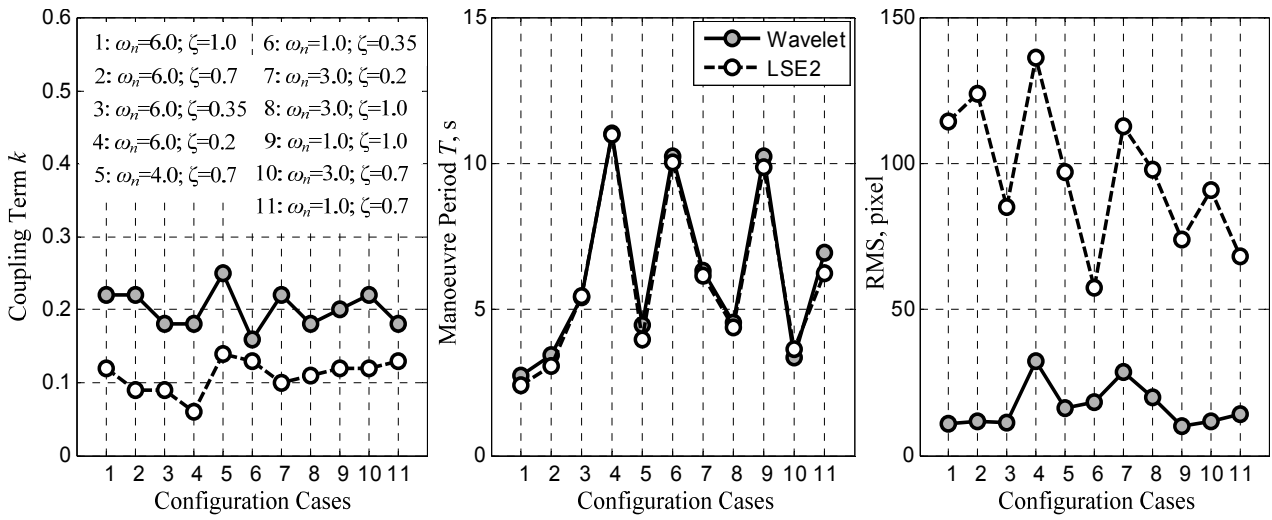


Fig. 18 Comparison of results from LSE2 and PWA approaches for ball test

Moreover, the first and fifth cases have been illustrated in Fig. 19 to show performance comparisons for these cases.

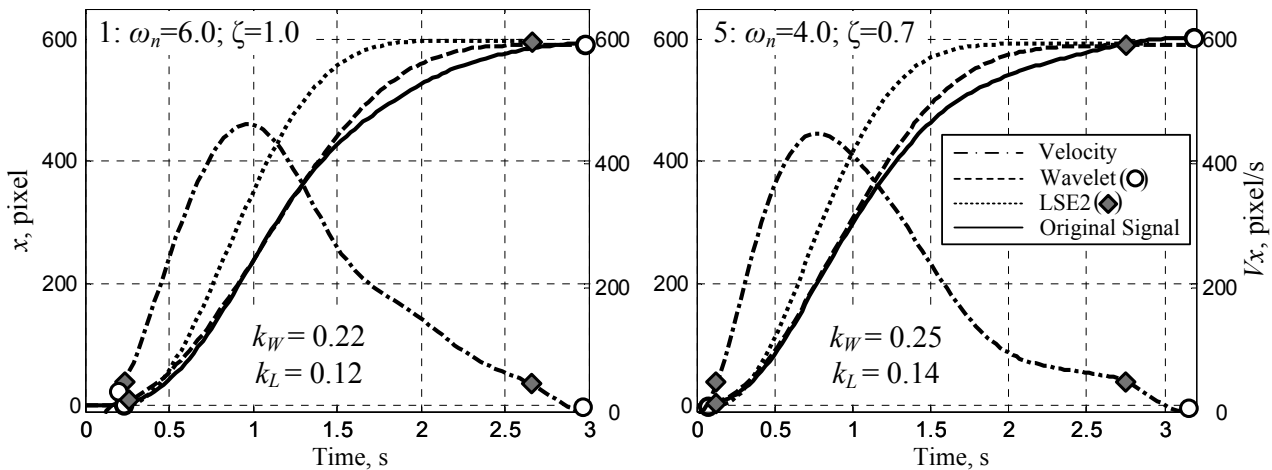


Fig. 19 Comparison of period selection and quality of fit for test cases 1 and 5

The k values (< 0.5) from both approaches in Fig. 18 indicate that the subject seem to adopt the similar control strategy moving the ball from left to right by electing to initiate the deceleration earlier, regardless of different dynamic system configurations. However, similar to the MTE cases discussed in the previous Section, the results in Fig. 18 show that the PWA approach achieves a smaller RMS error, compared with the LSE2 method. This is also reflected here in Fig. 19 with smaller gaps between the constructed signal from the PWA approach and the original signal than for the signal reconstructed from the LSE2 method. Therefore, the k values determined from the PWA approach appear to be more appropriate to serve the original purpose of the experiment, though the values from the LSE2 approach also appear to be self-consistent.

The velocity profiles shown in Fig. 19 appear to contain minor oscillations, especially for case 5. These oscillations can severely deteriorate the performance of the LSE2 approach, such as the poor fitting shown in these figures. Furthermore, they also make the selection of the T values quite tedious by selecting an appropriate cropping ratio of the peak velocity (i.e. extensive trial and error is required). Furthermore, the oscillations also result in difficulty in achieving good convergence of the optimisation algorithm. For the new PWA approach, the oscillations also have an influence in degrading the fitting performance with the original signal, as shown from the obvious fitting gaps in Fig. 19. However, compared with the previous

approach, it still shows better performance. Furthermore, no extra effort is required of the users to tune the peak velocity cropping ratio to achieve a better fit and convergence.

When the fluctuation in the shapes of the gaps and their velocities become more powerful, such as the case shown in Fig. 5b, it becomes harder for both approaches to fit the related desired curves in Fig. A1. The idea of guidance element proposed in this paper therefore has to be adopted. Besides, the case in Fig. 5b is actually selected from this experiment with the sluggish configuration ($\omega_n = 2.0$; $\zeta = 0.2$). The data also has been pre-filtered (0.5 Hz) to reduce the influence from the stabilisation function.

The previous approach can meet limitations when being applied on these divided guidance elements. For example, the first guidance element is hypothesised to be a constant acceleration guide. However, the end velocity of this period is 70 pixel/s, which is more than 40% of its peak velocity. The previous approach fails to deal with this situation with such limited information available. This resembles the situation illustrated in Fig. 5b. Therefore, the results for Fig. 5b with the previous approach are ignored here. By contrast, the new approach, based on shape fitting, can overcome this problem. In addition, this advantage facilitates its implementation in any part of a signal. The results, as well as the wholly reconstructed signal from four guidance elements, are shown in Fig. 20.

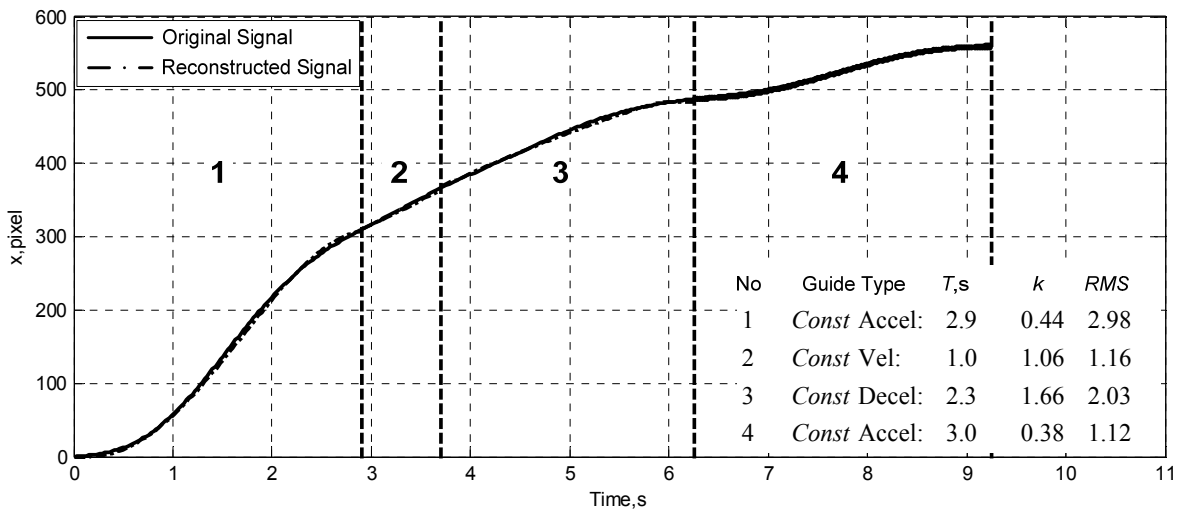


Fig. 20 Comparison the reconstructed signal from guidance elements with the original one

The original signal in Fig. 20 is plotted in the positive domain, not in the normalised negative form of Fig. 5 in which it is shown as the motion gap. However, their

shapes are exactly same. Moreover, the difference between the original signal and its reconstructed version from the four guidance elements is nearly

negligible. The good fit is also reflected in the very small RMS error values listed in the figure. The subject first follows a nearly perfect (symmetric) intrinsic constant acceleration that suggests a half period of acceleration followed by the other half of deceleration, according to the calculated k value (0.44) and the related curve (0.5) in Fig. A1(f). This period continues for around three seconds. Afterwards, the subject again follows a nearly perfect (flat) intrinsic constant velocity guide for around 1 second, by referring to the calculated k value (1.06) and the related curve (1.0) in Fig. A1(e). Then, the motion follows the constant deceleration intrinsic guide. The value $k = 1.66$ (or $\dot{\tau} = 0.83$ from Eq. (6)) indicates that the subject undertakes quite an aggressive control strategy [1;2]. Finally, the motion enters a constant acceleration guide phase again. The value $k = 0.38$ suggests the subject undertakes an early acceleration (in the time period being considered), and then slowly decelerates in order to stop before the desired goal is reached.

The final case shows a preliminary investigation of the new ideas presented in this paper. The results presented are encouraging in that the idea may possibly be extended to any guidance signal that can be decomposed into three basic guidance elements: constant acceleration guide, constant deceleration guide, and constant velocity guide. In other words, any guidance signal is a combination of these three elements. However, more work and effort is required to take the investigation further and to explore the points raised here.

5. Conclusions

Based on the results reported above, the following conclusions can be drawn;

- An alternative method, based upon positive wavelet analysis, that is constructed from the desired τ shapes has provided a better solution to calculate the τ -coupling term, k , when performing a τ -coupling analysis on a set of data.
- Compared with the previous approach, the k values from the newly developed approach present more numerical stability and reliability. Moreover, because of its supporting theory, the period, T , can be automatically determined. The new method removes trial and error or tuning processes used in the previous approach. In addition, it can deal with situations when only part of the required information is available.
- The concept of guidance elements has been preliminarily explored. The subject may adopt an adaptive guidance control strategy, not limited to follow one unique guide as traditionally assumed.

However, why the subject adopts an adaptive guidance strategy and what is the main triggering factor to change that control strategy are still not clear. These questions need to be pursued and clarified in future research.

Acknowledgements

The research reported in this paper was funded by The Aircraft and Rotorcraft Pilot Couplings - Tools and Techniques for Alleviation and Detection (ARISTOTEL, FP7-AAT-2010-RTD-1) from the European Community's Seventh Framework Programme (FP7/2007-2013) under grant agreement N° 266073.

Appendix

A. Derivations of τ -Guide Following Motion Forms

Table A1 Derivations of τ -Guide Following Motion Forms

Constant Deceleration Guide	Constant Velocity Guide <i>x_g motion</i>	Constant Acceleration Guide
$a_g = a_{g0}$	$a_g = 0$	$a_g = a_{g0}$
$v_g = v_{g0} + a_{g0} t$	$v_g = v_{g0}$	$v_g = v_{g0} + a_{g0} t$
$x_g = x_{g0} + v_{g0} t + \frac{a_{g0}}{2} t^2$	$x_g = x_{g0} + v_{g0} t$	$x_g = x_{g0} + v_{g0} t + \frac{a_{g0}}{2} t^2$
$x_g(T) = v_g(T) = 0$	$v_{g0} = -\frac{x_{g0}}{T}$	$v_{g0} = 0 \quad x_g(T) = 0$
$v_{g0} = -\frac{2x_{g0}}{T} \quad a_{g0} = \frac{2x_{g0}}{T^2}$	$a_{g0} = 0$	$a_{g0} = -\frac{2x_{g0}}{T^2}$
$x_g = x_{g0}(1-\hat{t})^2$	$x_g = x_{g0}(1-\hat{t})$	$x_g = x_{g0}(1-\hat{t}^2)$
$v_g = -\frac{2x_{g0}}{T}(1-\hat{t})$	$v_g = -\frac{x_{g0}}{T}$	$v_g = -\frac{2x_{g0}}{T}\hat{t}$
$\tau_g = -\frac{1}{2}(T-t) = \frac{1}{2}(2\tau_{g0}+t)$	$\tau_g = t - T = t + \tau_{g0}$	$\tau_g = -\frac{T}{2}\left(\frac{1}{\hat{t}} - \hat{t}\right)$
$\hat{t}_g = -\frac{1}{2}(1-\hat{t})$	$\hat{t}_g = -(1-\hat{t})$	$\hat{t}_g = -\frac{1}{2}\left(\frac{1}{\hat{t}} - \hat{t}\right)$
$\dot{\hat{t}}_g = \dot{\hat{t}}_g = 1$	$\dot{\hat{t}}_g = \dot{\hat{t}}_g = 1$	$\dot{\hat{t}}_g = \dot{\hat{t}}_g = \frac{1}{2}\left(1 + \frac{1}{\hat{t}^2}\right)$
<i>x motion</i>		
	$\tau_x = k \tau_g \quad x = C x_g^{1/k}$	
$\hat{x} = -(1-\hat{t})^{2/k}$	$\hat{x} = -(1-\hat{t})^{1/k}$	$\hat{x} = -(1-\hat{t}^2)^{1/k}$
$\dot{\hat{x}} = \frac{2}{k}(1-\hat{t})^{\left(\frac{2}{k}-1\right)}$	$\dot{\hat{x}} = \frac{1}{k}(1-\hat{t})^{\left(\frac{1}{k}-1\right)}$	$\dot{\hat{x}} = \frac{2\hat{t}}{k}(1-\hat{t}^2)^{\left(\frac{1}{k}-1\right)}$
$\ddot{\hat{x}} = -\frac{2}{k}\left(\frac{2}{k}-1\right)(1-\hat{t})^{2\left(\frac{1}{k}-1\right)}$	$\ddot{\hat{x}} = -\frac{1}{k}\left(\frac{1}{k}-1\right)(1-\hat{t})^{\left(\frac{1}{k}-2\right)}$	$\ddot{\hat{x}} = -\frac{2}{k}\left[\left(\frac{2}{k}-1\right)\hat{t}^2 - 1\right](1-\hat{t}^2)^{\left(\frac{1}{k}-2\right)}$
$\hat{t}_x = -\frac{k}{2}(1-\hat{t})$	$\hat{t}_x = -k(1-\hat{t})$	$\hat{t}_x = \frac{k}{2}\left(\hat{t} - \frac{1}{\hat{t}}\right)$
$\dot{\hat{t}}_x = \dot{\hat{t}}_x = \frac{k}{2}$	$\dot{\hat{t}}_x = \dot{\hat{t}}_x = k$	$\dot{\hat{t}}_x = \frac{k}{2}\left[1 + \left(\frac{1}{\hat{t}}\right)^2\right]$
$T = -\frac{2\tau_{x0}}{k}$	$T = -\frac{\tau_{x0}}{k}$	$T = -\sqrt{\frac{2x(0)}{k\ddot{x}(0)}}$

The motion gap, closure rate, and acceleration with constant deceleration, velocity, and acceleration guides with various different k values are plotted in Fig. A1. For consistent comparison, the k values are selected the same values for these three different guidance.

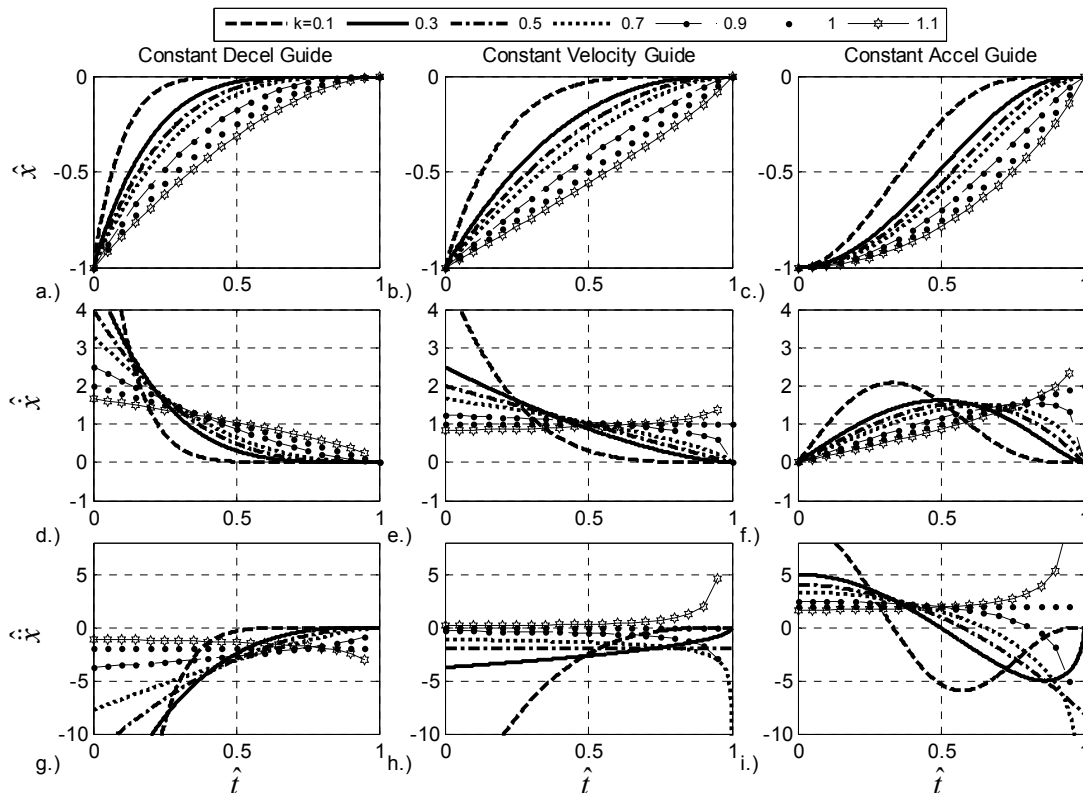


Fig. A1 Illustrations of motion gap, closure rate, and acceleration with constant deceleration, velocity and acceleration guide

References

- [1] Lee, D.N. Guiding movement by coupling τ s, *Ecological Psychology*, 1998, **10**, (3), pp. 221-250.
- [2] Padfield, G.D. *Helicopter Flight Dynamics*, 2nd ed., Blackwell Science, Oxford, 2007.
- [3] Padfield, G.D. The tau of flight control, *Aeronautical J*, Sept. 2011, 115, (1171), pp. 521-555.
- [4] Lee, D.N., Craig, C.M., and Grealy, M.A. Sensory and intrinsic coordination of movement, *Proc. of Biological sciences*, Jul. 1999, 266, (1432), pp. 2029-2035.
- [5] Lee, D.N., *Tau in Action in Development, Action as an Organizer of Learning and Development*, edited by. Rieser, J.J., Lockman, J.J., and Nelson, C.A. 33rd Volume in the Minnesota Symposium on Child Psychology, Minnesota, 2005, pp. 3-50.
- [6] Padfield, G.D., Lee, D.N., and Bradley, R. How do helicopter pilots know when to stop, turn or pull up?, *Journal of AHS*, 2003, 48, (2), pp. 108-119.
- [7] Padfield, G.D., Clark, G., and Taghizad, A. How long do pilots look forward? prospective visual guidance in terrain-hugging flight, *Journal of AHS*, 2007, 52, (2), pp. 134-145.
- [8] Jump, M., and Padfield, G.D. Investigation of the flare manoeuvre using optical τ , *J Guid Contr Dynam*, Sept.2006, 29, (5), pp. 1189-1200.
- [9] Jump, M., and Padfield, G.D. Progress in the development of guidance strategies for the landing flare manoeuvre using τ -based parameters, *Aircraft Eng Aero Tech*, 2006, 78, (1), pp. 4-12.
- [10] Clark G. *Helicopter Handling Qualities in Degraded Visual Environments (DVE)*, PhD Thesis, The University of Liverpool, UK, 2007.
- [11] Padfield G.D., Lu, L., and Jump, M. Tau guidance in boundary-avoidance tracking - new perspectives on pilot-induced oscillations, *J Guid Contr Dynam*, 2012, 35, (1), pp. 80-92.
- [12] Gilbert, S. *Linear Algebra and Its Applications*, 4th ed., Brooks Cole, California, United States, 2006.

- [13] Jones, J.G., and Watson, G.H. Multiresolution analysis using adaptive wavelets, In: *Wavelet Applications*, SZU, H.H. (Ed), Proc. SPIE, 1994, Orlando, FL, USA, 2242, pp. 119-129.
- [14] Watson, G.H., and Jones, J.G. Positive wavelet representation of fractal signals and images, In: *Applications of Fractals and Chaos*, 1993, Crilly, A.J., Earnshaw, R.A., and Jones, H.(Eds), Springer-Verlag Berlin Heidelberg, pp. 117-135.
- [15] Foster, G.W., and Jones, J.G. Analysis of atmospheric turbulence measurements by spectral and discrete-gust methods, *Aeronautical J*, May 1989, 93, pp. 162-176.
- [16] Gallant, J.C., and Hutchinson, M.F. Scale dependence in terrain analysis, *Mathematics and Computers in Simulation*, 1997, 43, (3), pp. 313-322.
- [17] Jones, J.G., Padfield, G.D., and Charlton, M.T. Wavelet analysis of pilot workload in helicopter low-level flying tasks, *Aeronautical J*, Jan.1999, 103, (1019), pp. 55-63.
- [18] Daubechies, I. *Ten Lectures on Wavelets*, 1st ed., SIAM: Society for Industrial and Applied Mathematics, 1992.
- [19] Meyer, M., and Padfield, G.D. First steps in the development of handling qualities criteria for a civil tilt rotor, *Journal of AHS*, 2005, 50, (1), pp.33-46.
- [20] Lee, D.N. A theory of visual control of braking based on information about time-to-collision, *Perception*, 1976, 5, (4), pp. 437-459.
- [21] Padfield, G.D., Charlton, M.T., Jones, J.G., Howell, S.E., and Bradley, R. Where does the workload go when pilots attack manoeuvres? an analysis of results from flying qualities theory and experiment, 20th European rotorcraft Forum, Amsterdam, Oct.4th -7th, 1994.
- [22] Anon. Aeronautical design standard performance specification handling qualities requirements for military rotorcraft ADS-33E-PRF. US Army Aviation and Missile Command, Aviation Engineering Directorate, Redstone Arsenal, Alabama, Mar. 2000.
- [23] Padfield, G.D., and White, M.D. Flight simulation in academia; HELIFLIGHT in its first year of operation, *Aeronautical J*, Sept. 2003, 107, (1075), pp. 529-538.
- [24] White, M.D., Perfect, P., Padfield, G.D., Gubbels, A.W., and Berrayman, A.C. Acceptance testing of a rotorcraft flight simulator for research and teaching: the importance of unified metrics, 35th European Rotorcraft Forum, Hamburg, Germany, Sept. 22th - 25th 2009.
- [25] Jones, M., Jump, M., Lu, L., Pavel, M., and Yilmaz, D. The Use of the Phase-Aggression Criterion for Identification of Rotorcraft Pilot Coupling Events, 38th European Rotorcraft Forum, Amsterdam, Netherlands, Sept. 4th-7th, 2012.